Basin Research (2004) **16**, 325–338, doi: 10.1111/j.1365-2117.2004.00235.x

Origin of the *in situ* stress field in south-eastern Australia

Mike Sandiford,* Malcolm Wallace* and David Coblentz†

**School of Earth Sciences, University of Melbourne, Victoria, Australia*
†*Los Alamos National Laboratory, Los Alamos, NM, USA*

ABSTRACT

The *in situ* stress field of south-eastern Australia inferred from earthquake focal mechanisms and bore-hole breakouts is unusual in that it is characterised by large obliquity between the maximum horizontal compressive stress orientation (S_{Hmax}) and the absolute plate motion azimuth. The evolution of the neotectonic strain field deduced from historical seismicity and both onshore and offshore faulting records is used to address the origin of this unusual stress field. Strain rates derived from estimates of the seismic moment release rate (up to $\sim 10^{-16}\,s^{-1}$) are compatible with Quaternary fault–slip rates. The record of more or less continuous tectonic activity extends back to the terminal Miocene or early Pliocene (10–5 Ma). Terminal Miocene tectonic activity was characterised by regional-scale tilting and local uplift and erosion, now best preserved by unconformities in offshore basins. Plate-scale stress modelling suggests the *in situ* stress field reflects increased coupling of the Australian and Pacific Plate boundary in the late Miocene, associated with the formation of the Southern Alps in New Zealand.

INTRODUCTION

It is widely recognised that continental *in situ* stress fields are the product of the interaction between tectonic forces acting along plate boundaries, tractions at the base of the plates and intraplate variations in density and rheology (Zoback *et al*., 1989; Zoback, 1992; Lithgow-Bertollini & Guynn, 2004). However, the relative control of each of these factors exerts on the observed stress regimes in continental interiors remains poorly understood. Since the configuration of plate boundaries is relatively well constrained, at least for the recent geological past, the neotectonic record within continental interiors should provide useful insights into the relative contributions of various plate boundary forces and intraplate sources of stress. In this contribution we focus on the neotectonic record in south-eastern Australia with reference to the origin of the stress field (Hillis & Reynolds, 2000).

One of the more intriguing features of the *in situ* stress field in the Indo-Australian plate is the disparity between the maximum horizontal compressive stress (S_{Hmax}) orientation and the absolute plate velocity azimuth; an observation that is at odds with the intraplate stress field within other, relatively fast moving, continental plates such as the North American and South American plates where S_{Hmax} is aligned with the absolute plate velocity azimuth (Sbar & Sykes, 1973; Zoback *et al*., 1989; Richardson, 1992; Zoback, 1992). The main feature of the S_{Hmax} orientations with the Indo-Australian plate is a broad arcuate trend from N–S in India, through E–W from the central Indian Ocean to the western Australian margin, to NE–SW in northern Australia (Fig. 1, Coblentz *et al*., 1998; Hillis & Reynolds, 2000). This trend is now well understood in terms of a balance between collisional torques along the Himalaya and Papua New Guinea plate boundary segments (that resist plate motion) and the plate driving torques associated with subduction ('slab-pull'), the cooling ocean lithosphere ('ridge-push') and tractions induced by the associated mantle flow(Coblentz *et al*., 1995, 1998; Sandiford *et al*., 1995; Lithgow-Bertollini & Guynn, 2004). Although this example illustrates the extremely important role played by boundary forces in the Indo-Australian intraplate stress field (Coblentz *et al*., 1995, 1998; Sandiford *et al*., 1995), there are other features of the intraplate stress field that remain enigmatic. In particular, the E–W to SE–NW orientation of S_{Hmax} in south-eastern Australia (Denham & Windsor, 1991; Hillis & Reynolds, 2000; Fig. 2) cannot easily be understood in terms of the balance between the plate driving forces and the collision zones along the northern plate boundary that resist plate motion.

Two distinct hypotheses have been proposed for the anomalous orientation of the *in situ* stress field in south-eastern Australia. Coblentz *et al*. (1995, 1998) and, more recently, Sandiford (2003a) have suggested that it relates to interactions along the Pacific–Australian plate boundary associated with the generation of the Southern Alps of New Zealand. In contrast, Zhang *et al*. (1996) have argued that broad E–W compression in eastern Australia results primarily from the density structure associated with the development of the eastern Australian margin, which

Correspondence: Mike Sandiford, School of Earth Sciences, University of Melbourne, Victoria 3010, Australia. E-mail: mikes@unimelb.edu.au

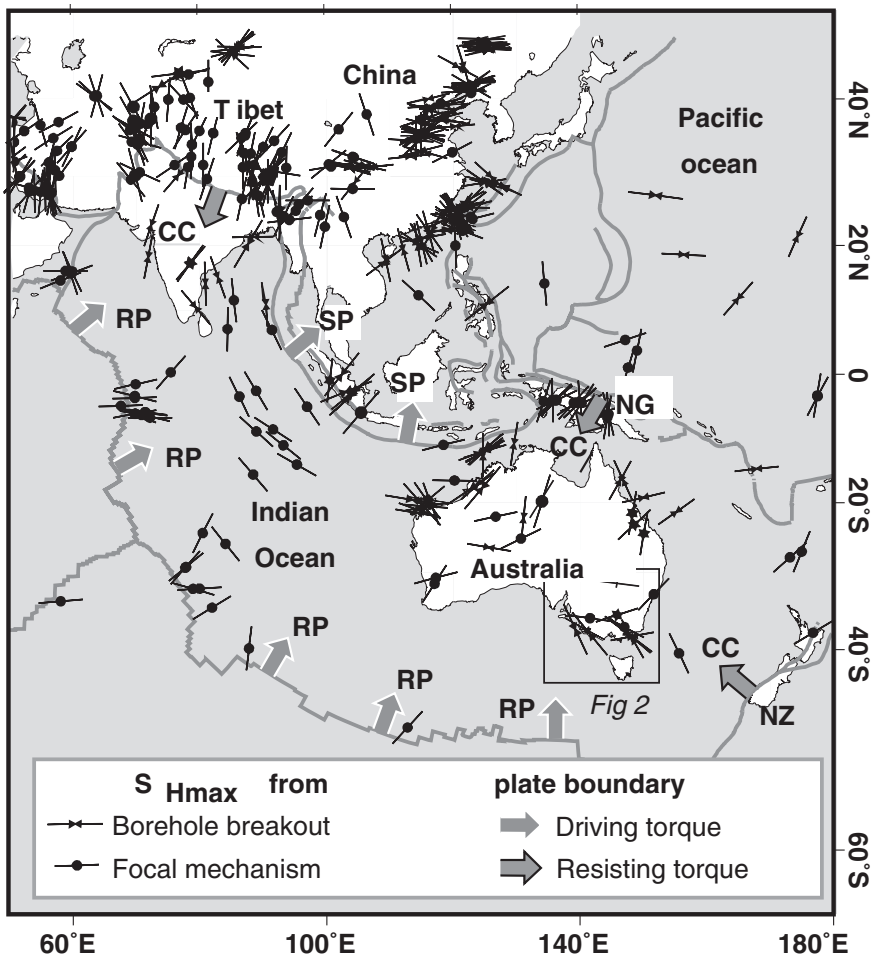

Fig. 1. Pattern of *in situ* stress in the Indo-Australian and neighbouring plates (after Zoback *et al*., 1989). Symbols for generalised plate sources of stress: RP, ridge push; SP, slab pull; CC, continental collision.

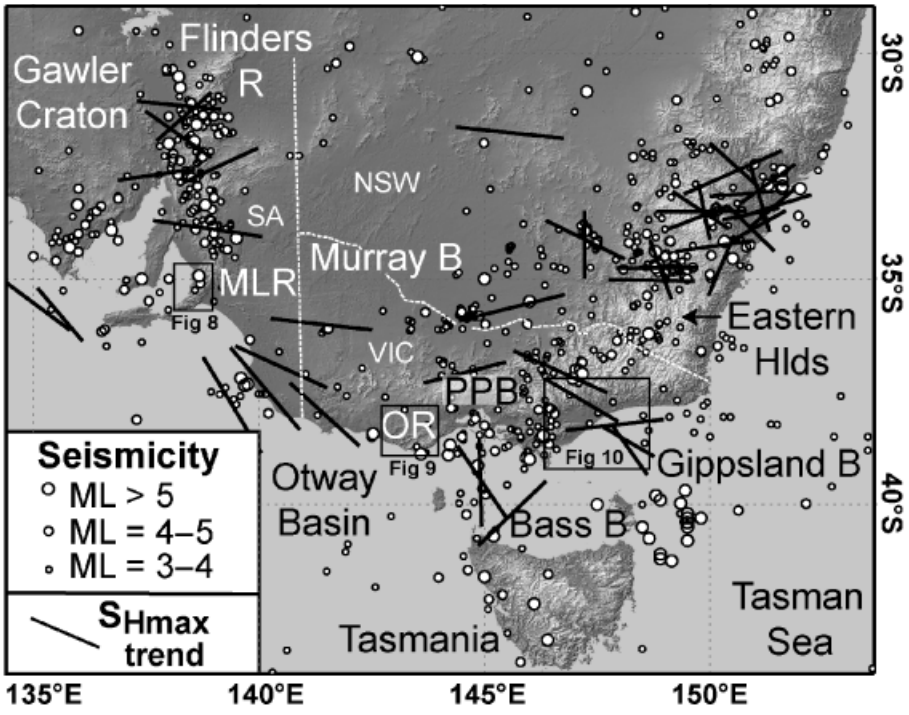

Fig. 2. Distribution of seismicity (Geoscience Australia earthquake database), topography and selected S_{Hmax} trends (after Hillis & Reynolds, 2000) in south-eastern Australia. OR, Otway Range; PPB, Port Phillip Bay; MLR, Mount Lofty Range. Boxes labelled Fig. 8, Fig. 9 and Fig. 10 show the position of Figs 8a, 9a and 10a, respectively.

exhibits a classic rift-related escarpment between the Eastern Highlands and a narrow coastal plain bordering the Tasman Sea (Fig. 2). Although the crustal density structure beneath the Eastern Highlands must undoubtedly influence the local stress regime it seems unlikely to account for the S_{Hmax} trends in southern Victoria and the

offshore basins further south (including the Gippsland, Bass and Otway Basins, Fig. 2), where there is no prominent coastal escarpment. The hypothesis that the *in situ* stress field in south-eastern Australia is primarily controlled by Pacific–Australian plate interactions associated with the generation of the Southern Alps of New Zealand is testable inasmuch as the Southern Alps have formed since the late Miocene due to an increase in convergence and/or coupling between the Pacific and Australian plates (Sutherland, 1996; Walcott, 1998).

In this contribution, we evaluate the role played by plate boundary forces in the evolution of the stress state in south-eastern Australia, using constraints provided by the neotectonic and stratigraphic record and insights gained from plate-scale stress modelling. The work builds on earlier studies involving the authors that provided an evaluation of the neotectonic record of south-eastern Australia (Dickinson *et al*., 2001, 2002; Sandiford, 2003a), and an analysis of the plate-scale stress distribution (Coblentz *et al*., 1995, 1998; Reynolds *et al*., 2002), wherein the reader can find far more detailed descriptions than provided here. A useful context for understanding the neotectonic record is provided by the modern-day deformation rates, and so we begin with a brief outline of constraints on the modern day seismic strain rates. This is followed by a summary of the results of numerical modelling of intraplate stress within the greater Indo-Australian plate. We then briefly summarise observations outlined elsewhere (Dickinson *et al*., 2001, 2002; Sandiford *et al*., 2003) showing that, despite its remote position with respect to active plate boundaries, the south-eastern part of the Australian continent contains a surprisingly rich record of late Neogene tectonic activity. This is followed by an outline of constraints on the timing, orientation and amplitude of this neotectonic activity. Finally we use these constraints to inform the debate concerning the origin of the *in situ* stress field in south-eastern Australia.

IN SITU STRESS AND SEISMICITY IN SOUTH-EASTERN AUSTRALIA

The nature of the *in situ* stress field in continental Australia is well documented by Hillis & Reynolds (2000), and here we simply summarise the observations pertinent to the south-east part of the continent (Fig. 2). Focal mechanisms for earthquakes in the Flinders Ranges yield a shortening direction of $83 \pm 30^\circ$ (Greenhalgh *et al*., 1994; Hillis & Reynolds, 2000). Using a formal inversion of six focal mechanisms from the Flinders Ranges, Clark & Leonard (2003) derived an S_{HMax} azimuth of 82° in a purely strike–slip stress regime. In the Eastern Highlands of Victoria and southern New South Wales, reverse focal mechanisms define a SE–NW shortening direction (Gibson *et al*., 1981). Clark & Leonard's (2003) inversion of four Eastern Highland earthquakes yields an S_{Hmax} azimuth of 315° in a purely reverse stress regime. Borehole breakout data from two basins along the south-eastern margin are sufficient to define a significant trend (Hillis & Reynolds, 2000). In the Otway Basin (Fig. 2), the azimuth of S_{Hmax} derived from breakouts is $136 \pm 15^\circ$, whereas in the Gippsland Basin near the south-eastern corner of the continent (Fig. 2) breakouts yield S_{Hmax} azimuths of $130 \pm 20^\circ$. Stress orientation data from borehole breakouts in the Bass Basin, between Victoria and Tasmania, are more scattered, and do not yield a statistically significant trend.

The south-east part of continental Australia is one of its most seismically active parts (Fig. 2), with a broad distribution of earthquakes up to $\sim M_{\mathrm{L}} = 6.4$ across a zone $\sim$1000 km in width from the eastern seaboard to the Gawler Craton in the west. Distinct concentrations in seismic activity occur in the Flinders Ranges–eastern Gawler Craton region of South Australia (the Flinders Seismic zone, FSZ), and in the belt trending from the west coast of Tasmania, through south-central Victoria, north-east through the Eastern Highlands into southern New South Wales (the south-eastern seismic zone, SESZ; Fig. 2). The intensity of seismic activity in these zones contrasts considerably with the intervening Murray Basin and the cratons to the west.

Seismic monitoring in the FSZ is sufficient for a more or less complete record down to local magnitude (M_{L}) 3 over the last 30 years (Gaul *et al*., 1990). Sandiford *et al*. (2003) provided quantitative estimates of seismic activity based on the familiar Gutenberg–Richter recurrence relation (Gutenberg & Richter, 1944):

$$\log(N) = a - bM$$

where N is the cumulative number of earthquakes greater than magnitude M. They derived a- and b-values of $\sim$3.0 and $\sim$1.0 for the Flinders Ranges (per 10 000 km^2, per year), implying relatively high degree of seismic activity for a stable continental interior (Johnston, 1994a). In contrast, the seismically much quieter Murray Basin has an a value less than 2, although Sandiford *et al*. (2003) note that the low level of seismicity in this region introduces considerable uncertainty in the estimation of a that could conceivably be as low as 1.7 for the basin as a whole or about 3% of the activity rate of the FSZ. Following Johnston (1994b), we can use these values to constrain the seismic moment release rate, from which we derive a notional seismic strain rate. The total seismic moment is

$$M_0 \approx \frac{1}{t}\left(\frac{b\left(10^{(a+d)}\right)}{c-b}\right)\left(10^{(c-b)}M_{\max}\right)$$

where t is the time span of the seismic record, $M_{\max}$ is the maximum-expected magnitude for earthquakes in the region of interest and c and d are factors that relate to the conversion of magnitude scale to seismic moment (Hanks & Kanamori, 1979):

$$\log(M_0) = cM + d.$$

In terms of the seismic moment, the seismic strain rate is (Kostrov, 1974):

$$\varepsilon_{xx} = \frac{1}{2\mu\nu} M_0$$

where μ is the Young's modulus (assumed here to be $8 \times 10^{10}\,\mathrm{N\,m^{-2}}$) and v is the volume of crust in which the seismicity occurs (we assume the seismogenic zone is 15 ± 5-km thick, based on the knowledge that the great majority of Australian earthquakes have epicentral depths less than 10 km, Gaul *et al.*, 1990).

Since the majority of the moment is carried by the largest, most infrequent earthquakes, the main uncertainty in the calculation of the seismic strain rates is the value of $M_{\max}$ (Fig. 3). For intraplate regions such as Australia with a historical record of only 200 years, it is extremely improbable that this record encompasses an earthquake of magnitude $M_{\max}$. The historical limit therefore provides a lower bound on $M_{\max}$. The largest instrumentally recorded earthquake in south-eastern Australia is $M_L \sim 6.4$. Elsewhere in Australia $M_L > 6.5$ quakes have occurred at a number of widely distributed localities, with the largest earthquake of magnitude $M_L = 6.8$ (in 1941, near Meeberrie in Western Australia). On longer timescales we would expect somewhat larger earthquakes, and thus the maximum earthquake-expected quake on geological timescales could conceivably be greater than $M_L \sim 7.0$. Assuming $M_{\max} = 7.0$, the seismic strain rate is $\sim 10^{-16}\,\mathrm{s^{-1}}$ for the FSZ (Fig. 3). The regional background deformation rate, defined in terms of seismicity of the Murray Basin, is less than $\sim 10^{-17}\,\mathrm{s^{-1}}$ (Fig. 3). Uncertainties in the a and b values, $M_{\max}$ ($\pm$ 0.25), the thickness of the seismogenic zone ($\pm$ 5 km) and Young's modulus yields large uncertainties in the seismic strain rate (of at least 50%). Our poor knowledge of seismic efficiency (i.e. the relative accommodation of strain by seismic and aseismic mechanisms), imply further uncertainty in translating seismically determined strain rates to bulk crustal strain rates (Johnston, 1994b). Nevertheless, these calculations provide an indication of the sorts of fault–slip to be expected if the present-day seismicity is indicative of longer-term geological strain rates. For example, a bulk strain rate of $10^{-16}\,\mathrm{s^{-1}}$ in uniaxial compression implies a total shortening of $\sim$250 mM yr^{-1} across the $\sim$100 km wide zone that encompasses the FSZ, which could be accounted for an ensemble of between 5 and 10 faults each accommodating between 25 and 50 m of horizontal slip per million years.

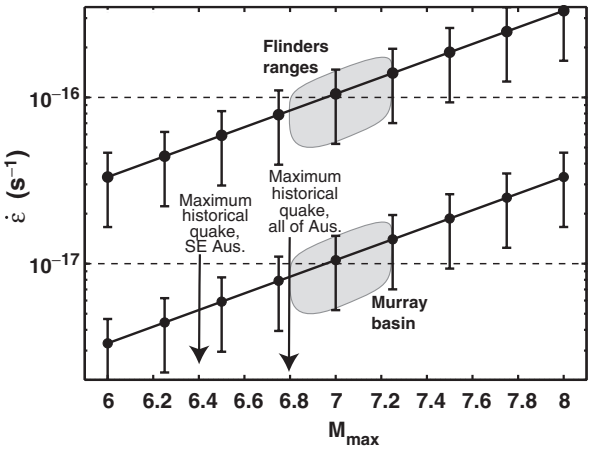

Fig. 3. Seismic strain rate estimates for the Flinders Ranges and Murray Basin as a function of maximum-expected earthquake magnitude ($M_{\max}$) – see text for discussion. Seismic activity data are derived from Sandiford *et al.* (2003). The seismogenic crust is assumed to be 15 ± 5-km thick. The grey shaded areas show the preferred seismic strain rate estimate. The data for the Murray Basin provide an upper bound to the seismogenic strain rate for the basin as a whole. Uncertainties in the seismic activity rate in the Murray Basin, stemming from the low levels of historical seismicity suggest that the seismogenic strain rate for the whole basin maybe as low as $\sim$30% of the rate shown here (i.e. order $10^{-18}\,\mathrm{s^{-1}}$).

INSIGHTS FROM PLATE-SCALE STRESS MODELLING

As noted in the Introduction, the *in situ* stress field throughout most of the Australian continent can be understood in terms of the interactions between the driving and resistive forces acting on the Indo-Australian plate (Coblentz *et al.*, 1995, 1998; Sandiford *et al.*, 1995; Reynolds *et al.*, 2002). The principal driving forces (see Fig. 1) include the so-called 'ridge-push' (associated with the long segment of ridges system along the southern boundary of the plate) and 'slab-pull' (associated with the subduction of oceanic lithosphere along its leading northern margin beneath Indonesia). The principal resistance is provided by the various convergent boundaries that produce a net collisional force acting on the plate particularly along the Himalayan, Papua New Guinea and, to a lesser extent, New Zealand boundary segments. The interaction between the driving and resisting boundary forces results in a high-angle alignment between S_{Hmax} and the collisional boundaries, resulting in broad arcs in S_{Hmax} through the plate that converge on central-eastern Australia. In this scenario, the E–SE orientation of S_{Hmax} in south-eastern Australia reflect its relative proximity to the New Zealand 'collision' (Fig. 1).

Inasmuch as the intraplate stress field can be understood in terms of present-day plate boundary configuration, we expect *a priori* that the stress field has evolved in response to changes in the plate boundaries; specifically in response to changes in the magnitude and orientation of the boundary forces acting on the plate margin. Convergence across the New Zealand segment of the Indo-Australian/Pacific plate margin has increased markedly over the Neogene, ultimately resulting in the 'collision zone' that has progressively built the Southern Alps starting possibly as early as 12 Ma (Sutherland, 1995, 1996), but certainly by 6.4 Ma (Walcott, 1998). The details of convergence can be reconstructed from relative plate velocity data. Here we use the rotation pole information of Walcott (1998) modified by Cande & Stock (2004). Vectors illustrating the change in the relative plate motion between the Pacific and Indo-Australian plates over the past 33 Ma (Chron 13) are

shown in Fig. 4. During this time interval the velocity of Pacific plate relative to the Indo-Australian plate has increased from about 23 to 41 m Myr^{-1} and changed in azimuth from an orientation of about 211° (measured clockwise from North) to about 250° (Fig. 4). The details of the relative plate motion between the Pacific and Indo-Australian plate at a location near the southern tip of the South Island of New Zealand (approximately 165°E, 47°S) over the last 33 Myr are listed in Table 2 and shown in Fig. 5. Between 33 and 6 Ma, the boundary normal velocity, or convergence, increased from less than 2 to ~14 m Myr^{-1}. From the past 6 Ma, the convergence rate appears to have stabilised at about 13 m Myr^{-1} (e.g. NUVEL-1A plate velocity data; DeMets *et al.*, 1994), although present-day GPS measurements (Drewes, 1998) indicate a much higher present-day convergence rate (23 m Myr^{-1}). The rotation pole data for the early Neogene (19 Ma) implies a convergence rate of ~9 m Myr^{-1}, equivalent to 70% late Neogene and NUVEL-1A rate or 38% of the present-day GPS rate.

The potential impact of changes in convergence across New Zealand on the orientation of the stress field in south-eastern Australia, maybe evaluated using a finite-element analysis of the intraplate stress field. The reference point for this analysis is provided by Reynolds *et al.* (2002) who deduced the plate boundary force ensemble that minimises the total misfit between the observed and predicted S_{Hmax} orientation across the entire Indo-Australian plate (Fig. 6a, note that all stress magnitudes are measures of the mean horizontal stress deviation from the lithostatic reference state, averaged over a 100-km-thick lithosphere). It should be noted that this analysis takes a plate-scale misfit measure between modelled and observed S_{Hmax} trends. As such it does not necessarily match stress regimes, and thus locally there are substantial discrepancies between predicted and observed stress regimes. For examples, in the Flinders Ranges the focal mechanisms imply a strike–slip stress regime, whereas the Reynolds *et al.* (2002) best-fit model predicts a reverse stress regime. Inasmuch as our objective here is to show how S_{Hmax} trends maybe influenced by changes in the forcing along a specific (New Zealand) plate boundary segment, the Reynolds *et al.* (2002) best-fit plate boundary ensemble provides a useful reference point, acknowledging that it may not necessarily provide the best possible solution for the *in situ* stress field in south-eastern Australia. This Reynolds *et al.* (2002) best-fit solution requires a compressional force of 3×10^{12} N m^{-1} along the New Zealand Southern Alps boundary segment (which encompasses the Puysegur Trench and Macquarie Ridge). Figure 6b shows the predicted intraplate stresses computed with no force acting across this boundary segment (with all other boundary forces as computed by Reynolds *et al.*, 2002). Figures 6 and 7 clearly show that plate convergence across New Zealand is capable of inducing a significant rotation in S_{Hmax} within south-eastern Australia. For the magnitude of the forces considered here, the S_{Hmax} in the vicinity of the Gippsland Basin varies in orientation from N22°E (in the absence of the convergent force) to N46°W (with a convergent force of 3×10^{12} N m^{-1}). Imposing the New Zealand boundary 'compression' also increases the magnitude of S_{Hmax} by almost 50% (see Table 3).

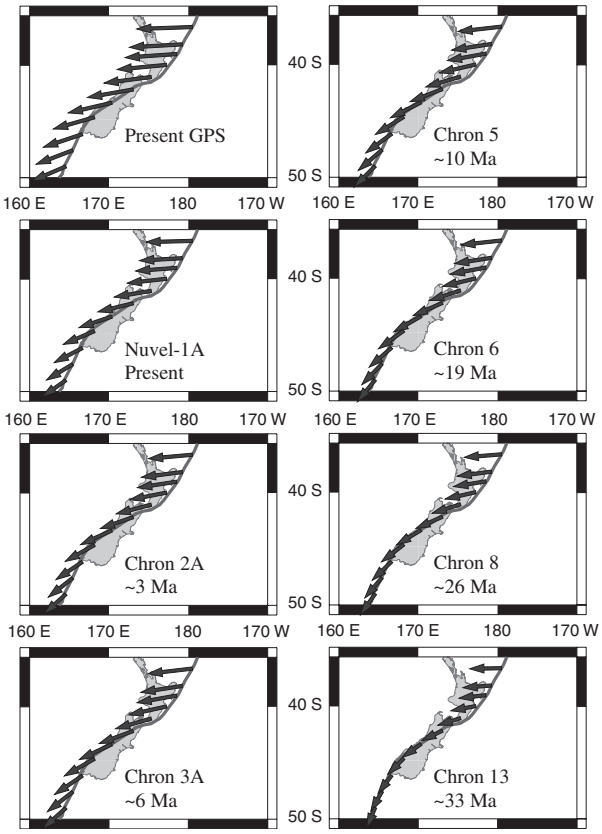

Fig. 4. Vectors illustrating the change in the relative plate motion between the Pacific and Indo-Australian plates since 33 Ma (Chron 13), derived from Cande & Stock (2004). The relative motion has changed from a predominately SW to EW orientation at the latitude of the South Island, New Zealand. For further information, see Table 2.

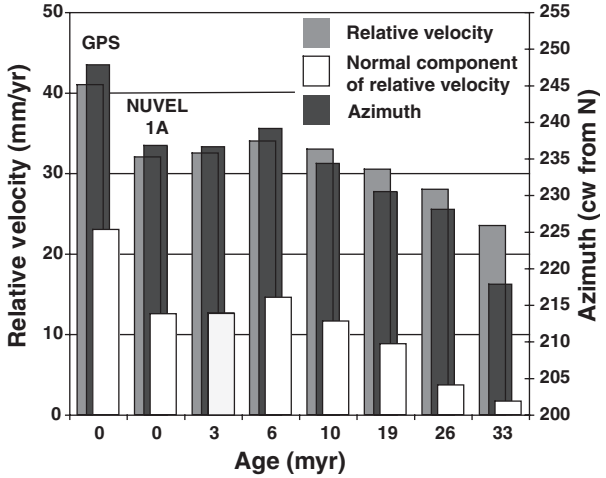

Fig. 5. Synopsis of the relative velocity of the Pacific plate relative to the Australian plate at a location presently at the southern tip of the South Island of New Zealand (165°E, 48°S). Rotation pole data (Table 2) are from Cande & Stock (2004).

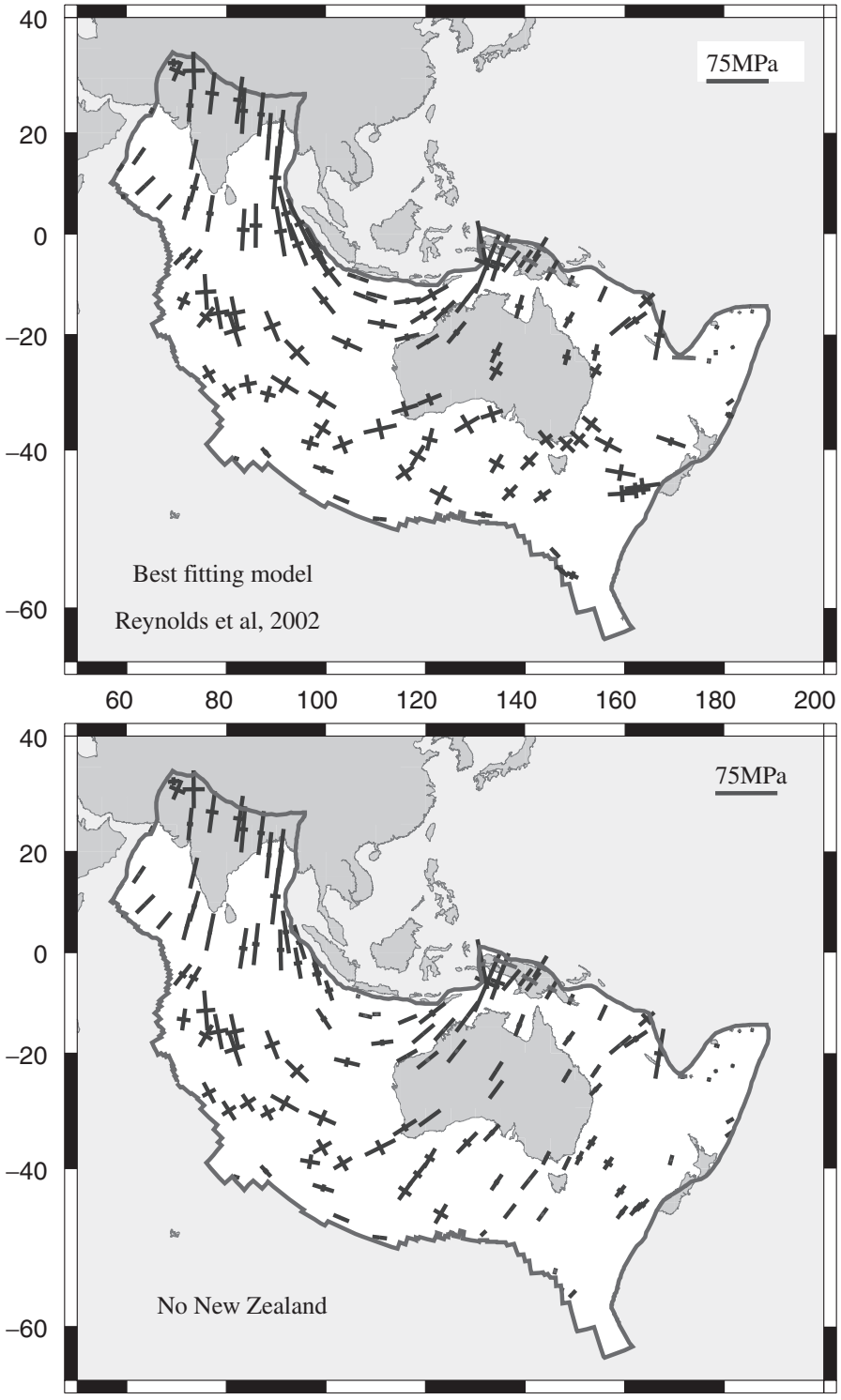

Fig. 6. (a) Best-fitting predicted intraplate stress field of the Indo-Australian plate Reynolds *et al.* (2002) and (b) the predicted stress field with contribution of New Zealand 'collisional' plate boundary forces removed. See Fig. 7 for more details of the modelling of the south-eastern Australian segment.

The way in which changes in convergence velocity across a boundary such as New Zealand impacts on the boundary force transmitted to the plate depends on the nature of the coupling across the boundary. A simplest possible scenario is a force, **F**, that scales linearly with convergence rate, $\boldsymbol{u}$, with the proportionality given by a coupling coefficient, c (i.e. $\mathbf{F} = c\boldsymbol{u}$). We assume a relatively high coupling coefficient since about 12 Ma, when the building of the Southern Alps began (Sutherland, 1995). Prior to 12 Ma there is no direct evidence for the accumulation of convergent strain in the form of mountain building, and hence the coupling is assumed to have been much weaker. Since the details of the coupling are subject of speculation, we approach the problem by considering bounds on the plausible extent of the coupling. We consider a lower bound with no coupling ($c = 0\,\mathrm{N\,s\,m^{-2}}$) and an upper bound provided by a linear scaling of the convergent velocities with the 'best-fit' force ($c \sim 3 \times 10^{6}\,\mathrm{N\,s\,m^{-2}}$). Plate rotation data summarised in Tables 1 and 2 indicate that the early Neogene (19 Ma) convergent velocity was, at

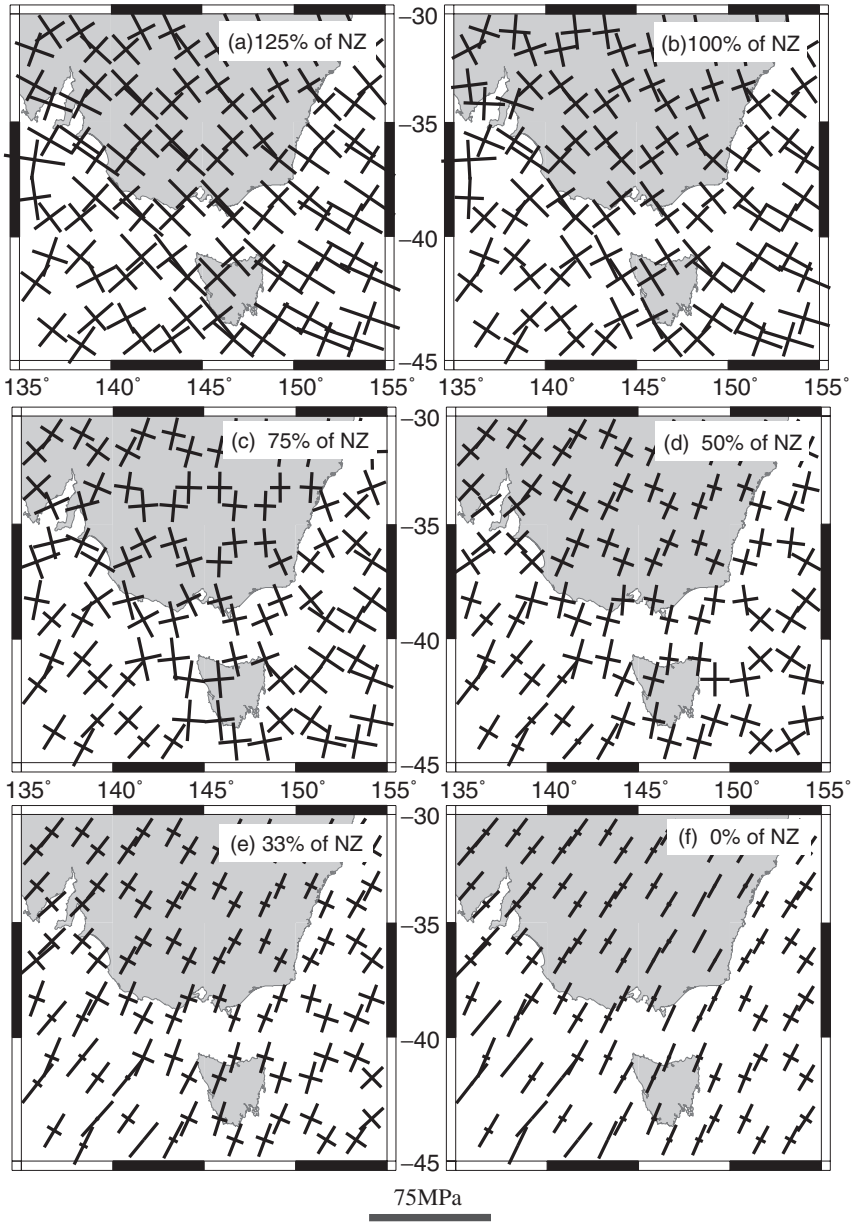

Fig. 7. Details of modelled stress in the south-eastern Australian region. The individual panels show the impact of reducing the magnitude of the New Zealand collisional force from 125% of the Reynolds *et al.* (2002) present-day 'best fit' model in (a) to 0% of the 'best-fit model' in (f). The best-fit solution is shown in (b). A stress scale of 75 MPa is shown at the bottom centre. Stress magnitudes are measured relative to the lithostatic reference state, averaged over a 100-km-thick lithosphere.

Table 1. Finite rotations of Australia relative to Pacific after Cande & Stock (2004).

Chron	Latitude (°N)	Longitude (°E)	Angle (deg. 10^{-7} yr^{-1})
GPS	65.7	2.9	10.7
NUVEL-1A	60.1	1.7	10.7
2A	58.8	4.3	10.73
3A	59.4	5.7	10.62
5	58.2	5.1	10.90
6	56.4	4.4	11.04
8	55.0	3.1	11.01
13	52.1	1.0	11.06

most, 70% of the present-day velocity, and possibly as little as 40% (depending on the merits of the NUVEL-1A and GPS velocity fields). Figure 7 shows details of the modelled stress in south-eastern Australian for a range of

Table 2. Summary of relative velocity data for Pacific plate motion relative to the Australian plate for a position at 165.45°E, 47.72°S (near the southern tip of New Zealand), based on rotation pole data in Table 1 (from Cande & Stock, 2004).

	Age (Ma)	Azimuth	Bound Ang	V (mm yr^{-1})	V_p (mm yr^{-1})
GPS	0	247.80	34.1	41.0	23.0
NUVEL-1A	0	236.80	23.1	32.0	12.6
2A	3	236.59	22.9	32.5	12.7
3A	6	239.09	25.4	34.0	14.6
5	10	234.34	20.6	33.0	11.6
6	19	230.47	16.8	30.5	8.8
8	26	228.04	7.7	28.0	3.8
13	33	217.84	4.2	23.5	1.7

Azimuth, the orientation of the relative plate motion vector (clockwise from North); bound ang, the angular difference between the relative plate motion vector and the current plate boundary; V, the absolute relative plate motion velocity; V_p, the component of V normal to the current plate boundary.

Table 3. Modelled stress parameters for a location in the Gippsland Basin (39.2°S, 148.3°E) as a function of the percentage of the present-day 'best-fit' New Zealand boundary force (3×10^{12} N m^{-1}, Reynolds *et al.*, 2002).

%	S_{Hmax}	S_{Hmin}	S_{Hmax} az	σ_{pp}	σ_{tt}	τ_{pt}	I_1
125	− 31.0	− 19.4	128.6	− 23.9	− 26.5	5.6	50.4
100	− 25.7	− 19.0	134.1	− 22.2	− 22.4	3.4	44.7
75	− 21.0	− 18.0	157.1	− 20.6	− 18.4	1.1	39.0
50	− 19.2	− 14.1	14.1	− 18.9	− 14.4	− 1.2	33.3
33	− 18.7	− 10.0	21.8	− 17.5	− 11.2	− 3.0	28.7
0	− 18.3	− 3.6	25.7	− 15.5	− 6.4	− 5.7	21.9

All stresses in MPa and represent deviations form the lithostatic reference state averaged over a 100-km-thick lithosphere. Negative values indicate compressional stress. S_{Hmax}, maximum horizontal stress; S_{Hmin}, minimum horizontal stress; S_{Hmax} az, azimuth of maximum horizontal stress measured clockwise from North; σ_{tt}, resolved longitudinal normal stress; τ_{pt}, resolved longitudinal shear stress; I_1, first invariant of the horizontal stress components.

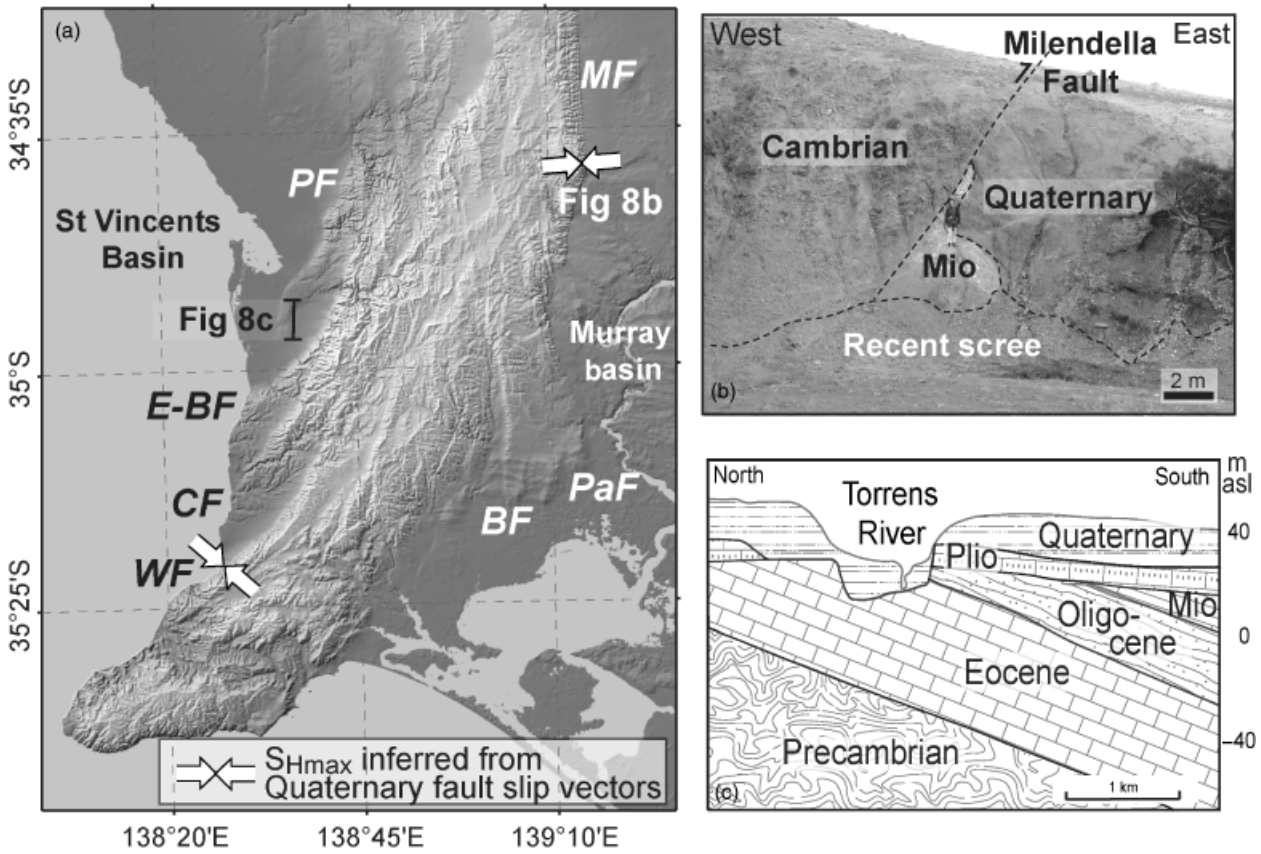

Fig. 8. (a) Shaded topography of the Mount Lofty Ranges highlighting the young, fault-bound nature of this landscape (see Fig. 2 for location). The main range bounding faults are the: Para (PF), Eden-Burnside (E-BF), Clarendon (CF), Willunga (WF), Bremer (BF), Palmer (PaF) and Milendella (MF) faults. (b) Outcrop of the Milendella Fault (location as shown in (a)). Reverse fault movement has thrust Cambrian metasedimentary sequences above Quaternary outwash gravels (~780 ka) and deformed and overturned early Miocene limestone (~20 Ma, Bourman & Lindsay, 1988). (c) N–S cross-section through township of Adelaide modified from Selby & Lindsay (1982) (location as shown in (a)) across the Para Fault block. The angular nature of the Miocene–Pliocene unconformity, implies significant titling of the Para Fault block in the late Miocene/early Pliocene. CF, Clinton Formation; SMS, South Maslin Sands; BPF, Blanch Point Formation; CGF, Chimamen Gully Formation; PWF, Port Willunga Formation; HCS, Hallet Cove Sandstone; HC, Hindmarsh Clay.

compressive boundary forces acting across the New Zealand boundary segment (from 125% to 0% of the 'best fit' present-day force). The modelled stress magnitude and orientation data for a location in the offshore Gippsland Basin (39.2°S, 148.3°E) are shown in Table 3. As summarised in Table 3, at ~70% of the present-day force, S_{Hmax} and S_{Hmin} are almost indistinguishable. At less than 70% of present-day force, the S_{Hmax} azimuth is in the NE quadrant, inconsistent with available *in situ* stress indicators.

The numerical modelling of the *in situ* stress field in south-east Australia summarised above, shows the importance of tractions associated with coupling across the Pacific–Australia plate boundary segment encompassing the New Zealand Southern Alps, the Puysegur Trench and

Macquarie Ridge. In the next section, we examine the late Neogene record of tectonic (neotectonic) activity to establish whether geological record is consistent with the hypothesis that the south-eastern Australian *in situ* stress field is controlled by changes in the Pacific–Australian plate coupling during the late Neogene.

THE LATE NEOGENE FAULTING RECORD IN SOUTH-EASTERN AUSTRALIA

The late Neogene record of south-eastern Australia contains abundant evidence for faulting. The intensity of this faulting shows marked spatial variation correlating, to a large extent, with the distribution of seismicity (Sandiford, 2003a). The most extensive faulting record occurs in the Flinders and Mount Lofty Ranges of South Australia, and in southern Victoria, in upland systems such as the Otway Range bordering the southern coastline (Fig. 2).

The Flinders and Mount Lofty Ranges in South Australia are bounded by N–S to NE–SW trending fault scarps, with the morphology of the Mount Lofty Ranges in particular providing dramatic testimony to the role of active faulting and formation of tilt blocks in shaping the large-scale landscape (Fig. 8a). Exposures of the main range-bounding faults bounding characteristically reflect reverse motion with a hanging wall of Proterozoic or Cambrian metamorphosed basement above a footwall comprising Quaternary conglomerates shed from the developing upland systems in the last ~1 Ma, and/or deformed late Palaeogene to early Neogene sedimentary successions deposited in the basins that now flank the uplands (Fig. 8b). Fault–slip kinematics are consistent with structures having formed in response to reverse stress regime with S_{Hmax} trending between 080°E and 125°E (Fig. 8a). The inferred S_{Hmax} azimuths are similar to those inferred from focal mechanism inversion (Clark & Leonard, 2003), although the reverse-fault stress regime inferred from known fault exposures contrasts the dominantly strike–slip regime inferred from most focal mechanism solutions. The cumulative post-Miocene displacement on the fault network that forms the western front of the Mount Lofty Ranges is estimated to be ~240 m (Sandiford, 2003a).

On the northern flanks of the Otway Range, in south-west Victoria, the remnants of an early Pliocene strandline system rise ~120 m over a series of ENE trending faults and monoclines to elevations of ~250 m (Fig. 9a and b). These strandlines, and correlatives in the Murray Basin, were developed during regression from an early Pliocene sea stand approximately 65-m high above present-day sea level (Brown & Stephenson, 1991) and thus imply ~200 m of uplift since the early to mid-Pliocene, accompanied by faulting. Basaltic volcanism associated with valley incision dates the faulting to 1–2 Ma (Sandiford, 2003b), in response to a stress regime with S_{Hmax} inferred to trend ~150° clockwise from north (Fig. 9a).

In the Gippsland Basin, in south-eastern Victoria, fold and joint patterns associated with late Miocene to early Pliocene structuring imply an NNW azimuth for S_{Hmax} (Barton, 1981), whereas *in situ* stress indicators have a NW azimuth (Fig. 10). This suggests the possibility of an anticlockwise rotation of ~20° in S_{Hmax} since the onset of Neogene deformation. Total slip on fault systems at this time exceeds 50 m based on the missing early Neogene section from beneath the Miocene–Pliocene unconformity. Many of the structures shown in Fig. 10 have continued to amplify through the late Pliocene into the Quaternary (Holdgate

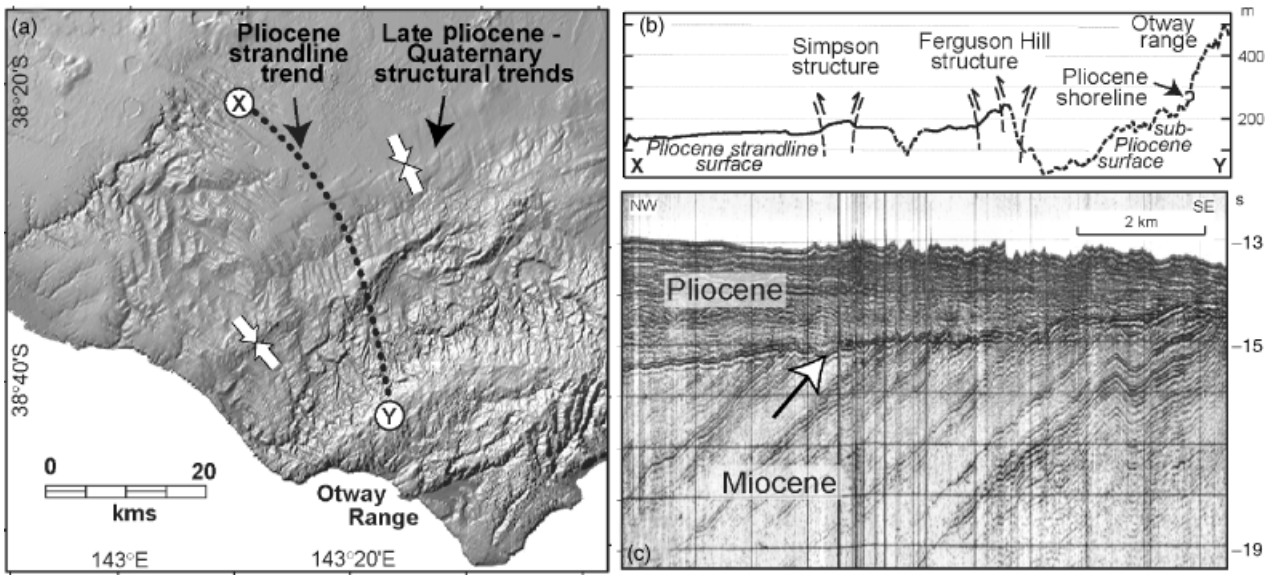

Fig. 9. (a) Shaded topography of the Otway Range region in south-west Victoria, showing deformation of Pliocene strandline system (see Fig. 2 for location). (b) Topographic profile along strandline system (*X*–*Y* in (a)) showing a general rise of over 100 m, on the north-west flank of the Otway Range, across a set of fault traces. (c) Shallow offshore seismic section south of the Otway Range, showing Miocene–Pliocene unconformity and folding of the underlying Miocene section along a NE trending axis.

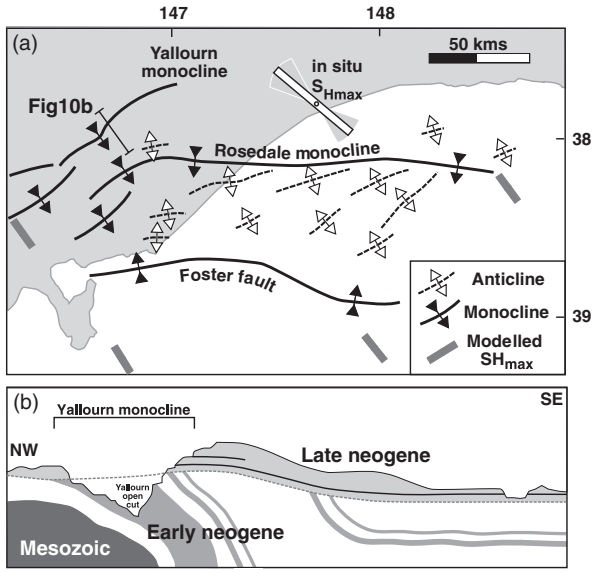

Fig. 10. Structure of the Gippsland Basin, south-eastern Victoria (see Fig. 2 for location). (a) Trace of major late Miocene to early Pliocene structures (after Barton, 1981). Grey bars are the modelled S_{Hmax} trends for the 'best-fit' model of Fig. 7b. The *in situ* S_{Hmax} orientation is $130 \pm 20^{\circ}$ (Hillis & Reynolds, 2000). (b) Section across the Yallourn monocline, in the Latrobe Valley. Approximately 50 m of coal-bearing (light grey) early Neogene section is missing from beneath the late Miocene–early Pliocene unconformity, beneath the Pliocene Haunted Hill gravels.

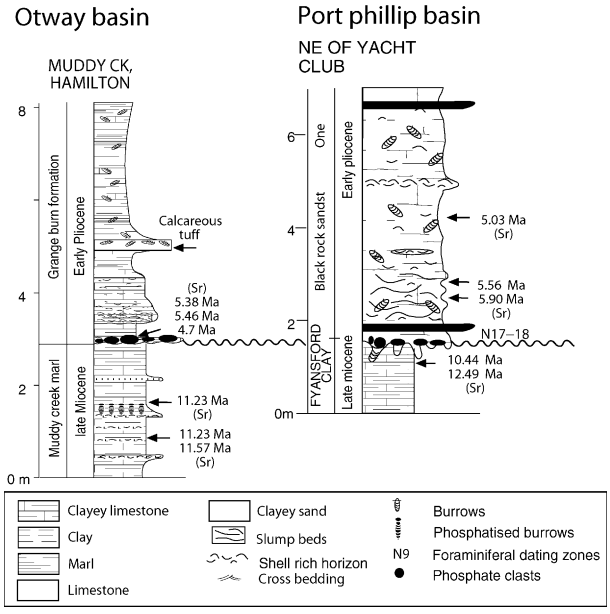

Fig. 11. Stratigraphic sections from the Otway and Port Phillip Basins that constrain the age of late Miocene tectonism and erosion (adapted from Dickinson *et al.*, 2002). Details of the strontium isotopic ages with errors are shown in Table 4.

et al., 2003), with a total late Neogene structural relief estimated to be several hundred metres.

The observations cited above suggest that the vertical component of the slip rates on the major active faults systems in south-eastern Australia exceeds several 10's m Myr^{-1} with an upper limit of $\sim$50 m Myr^{-1}, averaged over the last $\sim$5 Ma. Such slip rates compare favourably with the seismic shortening rates of the order of $\sim$150 m Myr^{-1} determined above. For example, range bounding faults in Mount Lofty Ranges and southern Victorian uplands slipping at $\sim$20 m Myr^{-1} on 60° dipping planes would account for $\sim$30% of the required seismic shortening. The active seismicity is quite widely distributed, especially across central-eastern Victoria, suggesting a broad zone of deformation is accommodating shortening in addition to the regions outlined above.

STRATIGRAPHIC CONSTRAINTS ON LATE NEOGENE TECTONISM IN SOUTH-EASTERN AUSTRALIA

The Oligocene to mid-Miocene sections in south-east Australian basins are dominated by cool-water carbonates reflecting the limited siliciclastic supply to the continental shelves and low continental erosion rates. Changes in the depositional regime at the Miocene–Pliocene boundary are indicated by an influx of siliciclastic sediments that, in most instances, unconformably overlie the older carbonates (Fig. 8c). This unconformity is best developed in near-shore and onshore positions, where the angularity is typically less than 5° but locally up to 90°. In St Vincents Basin, bordering the western Mount Lofty Range front, rotation on the Para Fault tilt block alone has excised $\sim$100 m of section prior to the Pliocene (Fig. 8a and c). In the Victorian basins, the Miocene and older sediments underlying the unconformity are commonly folded on NE–SW to ENE–WSW axes (Figs 9c and 10b, Dickinson *et al.*, 2002), reflecting generation under stress regimes with orientations similar to the *in situ* stress field. These relationships unequivocally implicate deformation, uplift and erosion of Miocene sediments prior to the Pliocene, although erosion of missing section has been augmented by contemporaneous eustatic sea-level changes, presumably associated with the Messinian low-sea stand (Carter, 1978; Roy *et al.*, 2000).

The timing of deformation is best constrained at localities where the least erosion of the underlying succession has occurred. In the Otway and Port Phillip Basins, the age of the youngest underlying Miocene succession is approximately 10.5–11.5 Ma whereas the age of the oldest overlying Pliocene section at these and other localities is approximately 5.5–6.0 Ma (Dickinson *et al.*, 2002; Fig. 11, Table 4). The onshore non-marine succession of the Gippsland Basin, in south-eastern Victoria, illustrates the profound influence of late Neogene tectonism on the sedimentary regime in south-eastern Australia (Fig. 10). In the onshore Gippsland Basin, Oligocene and Miocene brown coals underlie the Miocene–Pliocene unconformity, where at least 50 m of section has been locally removed in monoclinal structures that drape over basement reverse faults (Barton, 1981). The very low siliciclastic content of the brown coals implies very low continental erosion rates

Table 4. Measured $^{87}Sr/^{86}Sr$ ratios and calculated ages of molluscan carbonate material from stratigraphic sections shown in Fig. 11.

Location	Stratigraphic height (m)	$^{87}Sr/^{86}Sr$*	SE†	Age (Ma)‡	Lower age (Ma)	Upper age (Ma)
Hamilton	2.9	0.709023§	± 12	5.38	4.95	5.73
	2.9	0.709020§	± 12	5.46	5.04	5.77
	2.9	0.709045§	± 12	4.70	3.53	5.19
	1.6	0.708853§	± 12	11.23	10.61	12.08
	0.8	0.708853§	± 12	11.23	10.61	12.08
	0.8	0.708844§	± 12	11.57	10.91	12.61
Beaumaris	4.3	0.709036§	± 12	5.03	4.23	5.45
	2.8	0.709016§	± 12	5.56	5.15	5.82
	2.5	0.708995§	± 14	5.90	5.64	6.10
	1.7	0.708877	± 14	10.44	9.59	11.15
	1.7	0.708827	± 13	12.49	11.42	13.48

*All results are normalised to the SRM-987 standard = 0.710248 (Howarth & McArthur, 1997).
†Analytical uncertainty represents two standard errors of the mean of ~100 individual measurements and refers to the last two digits of the ratios.
‡Age calculated using Look-up table version 3: 10/99 (Howarth & McArthur 1997).
§Analyses recalculated from Dickinson *et al.* (2002).

during the Oligocene and Miocene. In contrast, an influx of quartz-rich gravels above the Miocene–Pliocene unconformity reflects an amalgam of tectonic events across the basin, as well as climatic changes that enhanced erosion rates (Bolger, 1991).

Stratigraphic relationships in southern Victoria imply significant generation of topographic relief in the terminal Miocene. For example, around the Otway Ranges, as much 600–1000 m of section has been removed from beneath the terminal Miocene unconformity (Dickinson *et al.*, 2001, 2002). In comparison with the ~200 m relief generated subsequent to the deposition of the Pliocene strandline system (Fig. 9), this suggests a peak in tectonic activity in the late Miocene (Fig. 11a).

The Miocene–Pliocene unconformity is generally absent from more seaward locations in the offshore basins. An exception occurs in the offshore Gippsland Basin, where anticlines initiated during early Eocene inversion (Brown, 1986; Johnstone *et al.*, 2001) continued to amplify by as much as several hundred metres in the late Miocene (Dickinson *et al.*, 2001). In the offshore Otway Basin, the position of the shelf edge and submarine canyon systems display a dramatic shift seaward at the Miocene–Pliocene boundary (Leach & Wallace, 2001), presumably in response to the combination of regional uplift and eustatic seal-level falls. Inversion in the Gippsland Basin apparently commenced in the early Eocene (at ~52 Ma), following a period of mild extension along NW–SE trending growth faults with NE–SW trending relay systems that linked the growth faults providing the main control for structural inversion (Johnstone *et al.*, 2001).

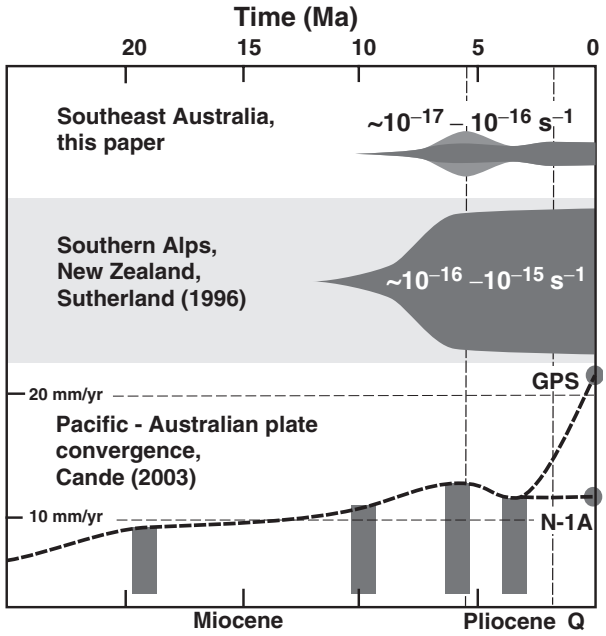

Fig. 12. Schematic summary of Neogene tectonic activity relevant to south-eastern Australia in relation to the Southern Alps (after Sutherland, 1996) and Australian–Pacific relative plate motion (after Cande & Stock, 2004).

DISCUSSION

The geological observations related to the active seismicity, and the Quaternary faulting and late Neogene stratigraphic records discussed above point to widespread, ongoing, low intensity neotectonic activity throughout south-eastern Australia that has substantially modified the landscape through the Quaternary and late Pliocene in a number of regions (most notably in the Flinders and Otway Ranges). Quaternary neotectonic structures yield palaeo-S_{Hmax} trends consistent with the *in situ* stress field as determined from active seismicity and bore-hole breakouts. Older late Miocene–early Pliocene activity in the Gippsland Basin, indicate the possibility of a slight anticlockwise rotation in S_{Hmax}, of about 20° to its present south-eastern azimuth. This neotectonic activity can be traced back to between 10 and 5 Ma, where it resulted in substantial, regional-scale tilting, now best preserved by regional unconformities in proximal offshore basins. These observations suggest that south-eastern Australia

preserves a neotectonic record of substantial displacement in the terminal Miocene, followed by ongoing deformation, possibly at somewhat lower bulk strain rates (Fig. 12, Dickinson *et al*., 2001, 2002; Sandiford, 2003a, b). The fact that neotectonic activity contains a more or less continuous record extending back to the latest Miocene connects the south-eastern Australia record with the record of the Southern Alps in New Zealand (Sutherland, 1996) and, in a more general sense, the relative rotation data for the Pacific and Australian plates (Walcott, 1998; Cande & Stock, 2004). However, there is only a weak connection between the timing of neotectonic activity in south-east Australia and the Australian–Pacific plate convergence rates, as deduced from the palaeo-rotation data of Cande & Stock (2004). These data suggest convergence rates increased by less than 25% between the early and late Neogene at the time (10–5 Ma) south-eastern Australia began to deform in a manner consistent with the *in situ* stress field. The geological history of the Southern Alps testify to significant changes in the coupling of the plates in southern New Zealand in this same period, and we hypothesise that it is the coupling between the Pacific and Australian plate motion, rather than convergence rate, that provides the major control on the stress regime and associated neotectonic strain field in south-eastern Australia during the late Neogene.

At present, the only observations pertaining to the nature of the palaeo-stress regime in south-eastern Australia prior to the late Miocene come from offshore basins (Johnstone *et al*., 2001). These observations, which relate to the timing of inversion of earlier formed growth faults, imply a transition from normal fault to stike–slip or reverse-fault stress regimes in the early Eocene. As noted by Sandiford *et al*. (1995) a critical change in plate configuration occurred in the early Eocene, when termination of spreading in the north-central Indian plates led to amalgamation of the Australian and Indian plates. Prior to this, the Australian plate was slow moving and bounded to a large degree by mid-ocean ridges in a configuration somewhat reminiscent of the modern African and Antarctic plates. As shown by Sandiford & Coblentz (1994) and Coblentz & Sandiford (1994), such plate boundary configurations are favourable to the development of extensional stress regimes, although not necessarily with stress magnitudes sufficient to engender extensional tectonics. The asymmetric disposition of plate boundaries following this amalgamation, more closely resembles other modern 'compressional' plates such as the North American and South American plates. The hypothesised change in south-eastern Australia at this time from a tectonic regime characterised by mild extension to inversion further corroborates the important role played by plate boundary effects in controlling the *in situ* stress field. However, in the past when the magnitude of the plate boundary forcing was lower, we might expect that sources of stress embedded within the plate, such as those associated with internal density variations, imposed a relatively greater spatial variability in the stress field.

The notion that the neotectonic record of south-eastern Australia reflects changes in the relative coupling of the Australian and Pacific plates has a number of important implications for understanding intraplate tectonics, as briefly summarised below:

1. It provides observational support for the results of numerical models (Coblentz *et al*., 1995, 1998) that suggest plate boundary interactions can propagate stresses 1000's of kilometres across the interior of plates (see also Zoback *et al*., 1989).
2. Conversely, it implies that the tectonic record of subtle deformation in continental interiors can provide important insights into far field plate boundary interactions. As shown here, intraplate deformation with associated relief generation of the order of 100 m can potentially augment the record of plate margin interaction, usually interpreted from regions much closer to the active plate boundaries.
3. The suggestion for south-eastern Australia is that the most substantial strain increments in intraplate settings relate to the change in intraplate stress regimes from one state to another. This is perhaps most easily interpreted in terms of an initial phase of accelerated deformation as pre-existing structures rearrange themselves with regard to the new stress field. An alternative possibility that this 'pulse' of deformation simply reflects the magnitude of the stress propagated into the plate during a phase of slightly increased plate convergence rates and associated coupling across New Zealand is not supported by the palaeo-stress data from the Gippsland Basin. Here, the evidence for an anticlockwise rotation of S_{Hmax} by $\sim 20^{\circ}$ implies, if anything, an increase in New Zealand forcing over time.

The distribution of historical seismicity across south-eastern Australia suggests that several factors are responsible for localising active deformation. Along the eastern and southern seaboards, in the SESZ, seismicity is concentrated in a zone $\sim$100–200 km inboard of the continental edge. Importantly, this zone strikes across the N–S to NNW–SSE structural grain inherited from Palaeozoic crustal growth. As such it would seem that the active deformation is localised by crustal scale processes associated with the formation of the present margin, rather than something inherited from the Palaeozoic. This pattern can be contrasted with the seismicity in the FSZ where the belt of seismicity defines a zone orthogonal to the present margin, and parallel to the inherited structural grain. Interestingly, this zone lies within a belt characterised by anomalously elevated heat flow ($\sim 80\,\mathrm{mW\,m^{-2}}$) related to exceptional heat-producing element concentrations in Proterozoic basement rocks (Neumann *et al*., 2000). Although it seems clear that seismicity here relates to fundamental weakness in the crust, it remains to be determined whether this weakness arises primarily from the pre-existing structural anisotropy or elevated thermal regimes associated with the high heat flows.

ACKNOWLEDGEMENTS

We acknowledge the constructive reviews of Mark Tingay and Balz Grollimund.

REFERENCES

Barton, C.M. (1981) Regional stress and structure in relation to brown coal open cuts of the Latrobe Valley, Victoria. *J. Geol. Soc.Aust.*, **28**, 333–339.

Bolger, P.F. (1991) Lithofacies variations as a consequence of late Cainozoic tectonic and palaeoclimatic events in the onshore Gippsland Basin. In: *The Cainozoic in Australia: A Re-Appraisal of the Evidence* (Ed. by M.A.J. Williams, P. DeDeckker & A.P. Kershaw), *Geol. Soc. Aust., Spec. Publ.*, **18**, 158–180.

Bourman, R.P. & Lindsay, J.M. (1988) Timing extent and character of late Cainozoic faulting on the eastern margin of the Mount Lofty Ranges, South Australia. *Trans. R. Soc. South Aust.*, **113**, 63–67.

Brown, B.R. (1986) Offshore Gippsland Silver Jubilee. In: *Second South-Eastern Australia Oil Exploration Symposium, Melbourne* (Ed. by R.C. Glenie), pp. 29–56. The Petroleum Exploration Society of Australia Victoria and Tasmanian Branch, Canberra, Australia.

Brown, C.M. & Stephenson, A.E. (1991) Geology of the Murray basin. *Aust. Bur. Miner. Resour.*, **235**, 430pp.

Cande, S.C. & Stock, J.M. (2004) Pacific–Antarctic–Australia motion and the formation of the Macquarie plate. *Geophys. J. Int.*, **157**, 399–414.

Carter, A.N. (1978) Phosphatic nodule beds in Victoria and the late Miocene–Pliocene eustatic event. *Nature*, **276**, 258–259.

Clark, D. & Leonard, M. (2003) Principal stress orientations from multiple focal-plane solutions: new insight into the Australian intraplate stress field. In: *Evolution and Dynamics of the Australian Plate* (Ed. by R.R. Hillis & D. Muller), *Geol. Soc. Aust., Spec. Publ.*, **22**, 91–106.

Coblentz, D. & Sandiford, M. (1994) Tectonic stress in the African plate: constraints on the ambient stress state. *Geology*, **22**, 831–834.

Coblentz, D.D., Sandiford, M., Richardson, R.M., Zhou, S. & Hillis, R.R. (1995) The origins of the intraplate stress field in continental Australia. *Earth Planet. Sci. Lett.*, **133**, 299–309.

Coblentz, D.D., Zhou, S., Hillis, R.R., Richardson, R.M. & Sandiford, M. (1998) Topography, boundary forces, and the Indo-Australian intraplate stress field. *J. Geophys. Res.*, **103**, 919–931.

DeMets, C., Gordon, G., Argus, D. & Stein, S. (1994) Effect of recent revisions to the geomagnetic reversal time scale on estimates of current plate motions. *Geophys. Res. Lett.*, **21**, 2191–2194.

Denham, D. & Windsor, C.R. (1991) The crustal stress pattern in the Australian continent. *Explor. Geophys.*, **22**, 101–106.

Dickinson, J.A., Wallace, M.W., Holdgate, G.R., Daniels, J., Gallagher, S.J. & Thomas, L. (2001) Neogene tectonics in SE Australia: implications for petroleum systems. *APEA J.*, **41**, 37–52.

Dickinson, J.A., Wallace, M.W., Holdgate, G.R., Gallagher, S.J. & Thomas, L. (2002) Origin and timing of the Miocene–Pliocene unconformity in south-eastern Australia. *J. Sediment. Res.*, **72**, 317–332.

Drewes, H. (1998) Combination of VLBI, SLR and GPS determined station velocities for actual plate kinematic and crustal deformation models. In: *Geodesy on the Move, IAG Symposia* (Ed. by R. Forsberg, M. Feissel & R. Dietrich), pp. 377–382. Springer-Verlag, Berlin.

Gaul, B.A., Michael-Leiba, M.O. & Rynn, J.M.W. (1990) Probabilistic earthquake risk maps of Australia. *Aust. J. Earth Sci.*, **37**, 169–187.

Gibson, G., Wesson, V. & Cuthberstson, R. (1981) Seismicity in Victoria to 1980. *J. Geol. Soc. Aust.*, **28**, 341–356.

Greenhalgh, S.A., Love, D., Malpas, K. & McDougall, R. (1994) South Australian earthquakes, 1980–1992. *Aust. J. Earth Sci.*, **41**, 483–495.

Gutenberg, B. & Richter, C.F. (1944) Frequency of earthquakes in California. *Bull. Seismol. Soc. Am.*, **25**, 185–188.

Hanks, T.C. & Kanamori, H. (1979) A moment-magnitude scale. *J. Geophys. Res.*, **84**, 2348–2350.

Hillis, R.R. & Reynolds, S.D. (2000) The Australian stress map. *J. Geol. Soc., London*, **157**, 915–921.

Holdgate, G.R., Wallace, M.W., Gallagher, S.J., Smith, A.J., Keene, J.B., Moore, D. & Shakif, S. (2003) Plio-Pleistocene tectonics and eustasy in the Gippsland Basin, southeastern Australia: evidence from magnetic imagery and marine geological data. *Aust. J. Earth Sci.*, **50**, 37–52.

Howarth, R.J. & McArthur, J.A. (1997) Statistics for strontium isotope stratigraphy: a robust LOWESS fit to the marine Sr-isotope curve for 0 to 206 Ma, with Look-up Table for derivation of numeric age. *J. Geol.*, **105**, 441–456.

Johnston, A.C. (1994a) The stable continental region earthquake database. The earthquakes of stable continental regions, 1. Assessment of large earthquake potential, Report TR-102261-1, Electric Power Research Institute, Palo Alto, CA, pp. 3-1–3-80.

Johnston, A.C. (1994b) Seismotectonic interpretations and conclusions from the stable continental region seismicity database. The earthquakes of stable continental regions, Report TR-102261-1, Electric Power Research Institute, Palo Alto, CA, pp. 4-1–4-102.

Johnstone, E.M., Jenkins, C.C. & Moore, M.A. (2001) An integrated structural and palaeogeographic investigation of Eocene erosional events and related hydrocarbon potential in the Gippsland basin. In: *Eastern Australian Basins Symposium 2001* (Ed. by K.C. Hill & T. Bernecker), *Petrol. Soc. Aust., Spec. Publ.*, 403–412.

Kostrov, B.V. (1974) Seismic moment and energy of earthquakes, and seismic flow of rocks. *Izv. Acad. Sci., USSR, Phys. Solid Earth*, **1**, 23–40.

Leach, A.S. & Wallace, M.W. (2001) Cenozoic submarine canyon systems in cool water carbonates from the Otway Basin, Victoria, Australia. In: *Eastern Australian Basins Symposium, A Refocused Energy Perspective for the Future* (Ed. by K.C. Hill & T. Bernecker), *Petrol. Explor. Soc. Aust., Spec. Publ.*, 465–473.

Lithgow-Bertelloni, C. & Guynn, J.H. (2004) Origin of the lithospheric stress field. *J. Geophys. Res.*, **109**, B01408, 10.1029/2003JB002467.

Neumann, N., Sandiford, M. & Foden, J. (2000) Regional geochemistry and continental heat flow: implications for the origin of the South Australian heat flow anomaly. *Earth Planet. Sci. Lett.*, **183**, 107–120.

Reynolds, S.D., Coblentz, D.D. & Hillis, R.R. (2002) Tectonic forces controlling the regional intraplate stress field in continental Australia: results from new finite-element modelling. *J. Geophys. Res.*, **107**, B7, 10.1029/2001JB000408.

Richardson, R.M. (1992) Ridge forces, absolute plate motions and the intraplate stress field. *J. Geophys. Res.*, **97**, 11739–11748.

Roy, P.S., Whitehouse, J., Cowell, P.J. & Oakes, G. (2000) Mineral sand occurrences in the Murray basin, south-eastern Australia. *Econom. Geol.*, **95**, 1107–1128.

Sandiford, M. (2003a) Neotectonics of south-eastern Australia: linking the Quaternary faulting record with seismicity and *in situ* stress. In: *Evolution and Dynamics of the Australian Plate* (Ed. by R.R. Hillis & D. Muller), *Geol. Soc. Aust., Spec. Publ.*, **22**, 107–120.

Sandiford, M. (2003b) Geomorphic constraints on the late Neogene tectonics of the Otway Range. *Aust. J. Earth Sci.*, **50**, 69–80.

Sandiford, M. & Coblentz, D. (1994) Plate-scale potential energy distributions and the fragmentation of ageing plates. *Earth Planet. Sci. Lett.*, **126**, 143–159.

Sandiford, M., Coblentz, D. & Richardson, R.M. (1995) Focusing ridge-torques during continental collision in the Indo-Australian plate. *Geology*, **23**, 653–656.

Sandiford, M., Leonard, M. & Coblentz, D. (2003) Geological constraints on active seismicity in southeast Australia. In: *Earthquake Risk Mitigation* (Ed. by J.L. Wilson, N.K. Lam & G. Gibson), *Aust. Earthquake Eng. Soc.*, 1–10.

Sbar, M.L. & Sykes, L.R. (1973) Contemporary compressive stress and seismicity in eastern North America: an example of intra-plate tectonics. *Geol. Soc. Am., Bull.*, **84**, 1861–1882.

Selby, J. & Lindsay, J.M. (1982) Engineering geology of the Adelaide city area. *South Aust. Geol. Survey Bull.*, **51**, 121 p.

Sutherland, R. (1995) The Australian–Pacific boundary and Cenozoic plate motions in the SW Pacific: some constraints from Geosat data. *Tectonics*, **14**, 819–831.

Sutherland, R. (1996) Transpressional development of the Australia–Pacific boundary through southern South Island, New Zealand: constraints from Miocene–Pliocene sediments, Waiho-1 borehole, South Westland. *NZ J. Geol. Geophys.*, **39**, 251–264.

Walcott, R.I. (1998) Modes of oblique compression: late Cenozoic tectonics of the South Island of New Zealand. *Rev. Geophys.*, **36**, 1–26.

Zhang, Y., Scheibner, E., Ord, A. & Hobbs, B.E. (1996) Numerical modelling of crustal stresses in the Eastern Australian passive margin. *Aust. J. Earth Sci.*, **43**, 161–175.

Zoback, M.L., Zoback, M.D., Adams, J., Assumpcao, M., Bell, S., Bergman, E.A., Blumling, P., Bereton, N.R., Denham, D., Ding, J., Fuchs, K., Gay, N., Gregersen, S., Gupta, H.K., Gvishiani, A., Jacob, K., Klein, R., Knoll, P., Magee, M., Mercier, J.L., Muller, B.C., Paquin, C., Rajendran, K., Stephansson, O., Suarez, G., Suter, M., Udias, A., Xu, Z.H. & Zhizhin, M. (1989) Global patterns of tectonic stress. *Nature*, **341**, 291–298.

Zoback, M.L. (1992) First- and second-order patterns of stress in the lithosphere: the world stress map project. *J. Geophys. Res.*, **97**, 11703–11728.

Manuscript received: 27 November 2003; Manuscript accepted: 28 May 2004

